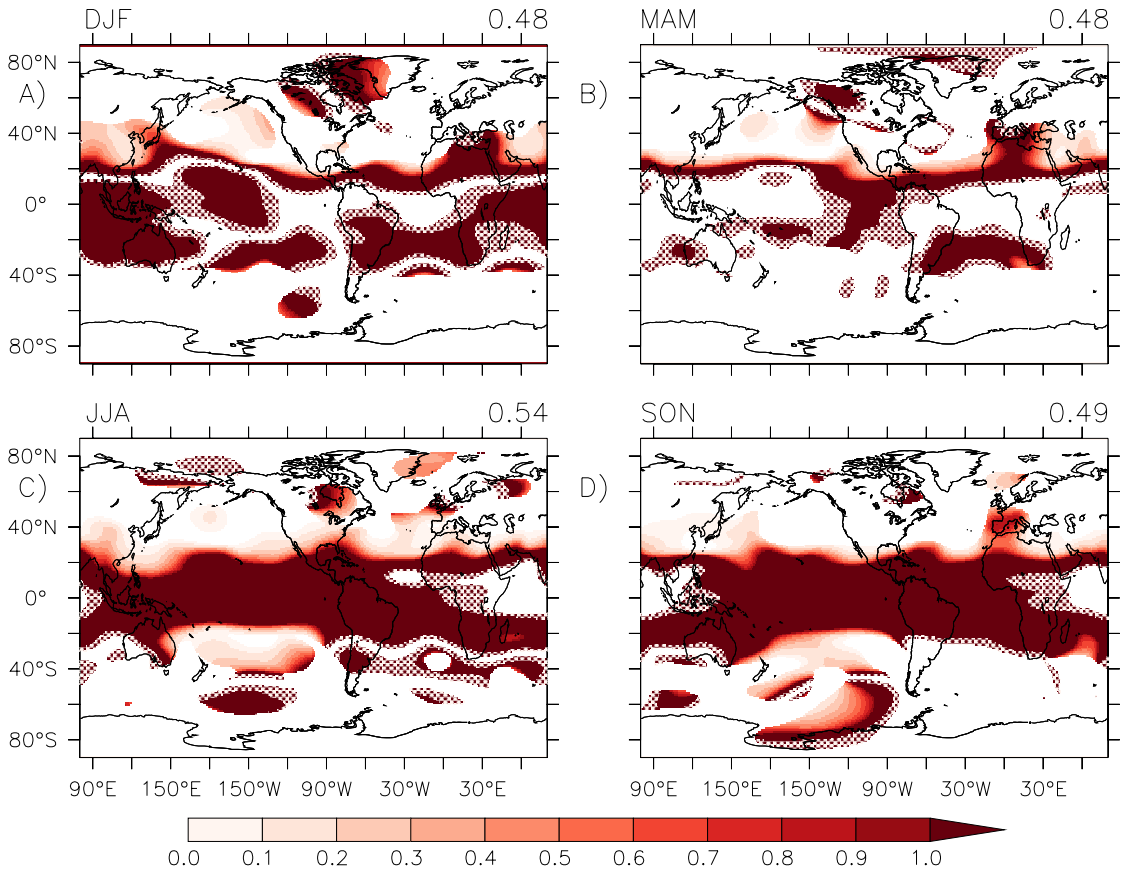


**Fig. 12** As Fig. 9, but for 500 hpa geopotential height (zg)

to reduced SST biases. The resulting sharper SST gradients can significantly influence the overlying atmosphere (Minobe et al. 2008; Parfitt et al. 2016). The increase of model resolution can also lead to changes in the variability of ocean models (Hodson and Sutton 2012; Jackson et al. 2020).

All these aspect demonstrate that increasing horizontal resolution in climate model studies can lead to changes in the mean climate state. For some processes, model climate may change or improve continuously with increasing resolution (Demory et al. 2014), for other processes changes may occur as a critical resolution threshold is passed after which key processes are explicitly resolved, for example atmospheric convection (Fosser et al. 2015), ocean eddies (He et al. 2018), or Rossby radius (Hewitt et al. 2016). These impacts of increasing climate on model resolution suggest that the response of the climate to the AMV may also vary with resolution. We attempt to address this question in the following section.

Experiments were performed at both high and low atmosphere resolution, but examination of Table 1 shows that comparing model resolution between models is dependent on how resolution is defined, due to the variation in grid geometries. It is also clear that there is no resolution threshold that divides the models into low and high resolution. This spread of model resolutions presents a challenge to assessing the impact of model resolution on the AMV response.

The change in the modelled AMV response due to resolution can be best expressed as a quadrature:

$$D_m = (X_+^H - X_-^H) - (X_+^L - X_-^L) \tag{4}$$

that is, the difference between the AMV response in the higher resolution models, and the AMV response in the lower resolution models. We can then propose two hypotheses:

1. $D_m$ is proportional to, or monotonic with the change in resolution $R_m$ $(=R^H - R^L)$
2. $D_m$ is zero unless the low and high resolution models span a critical resolution threshold, $R_c$

We can examine these hypotheses using the ANOVA test for $G_{er}$ (Eq. 3). If $G_{er}$ is not a significant factor ($p < 0.05$), then we are unable to reject the null hypotheses that the

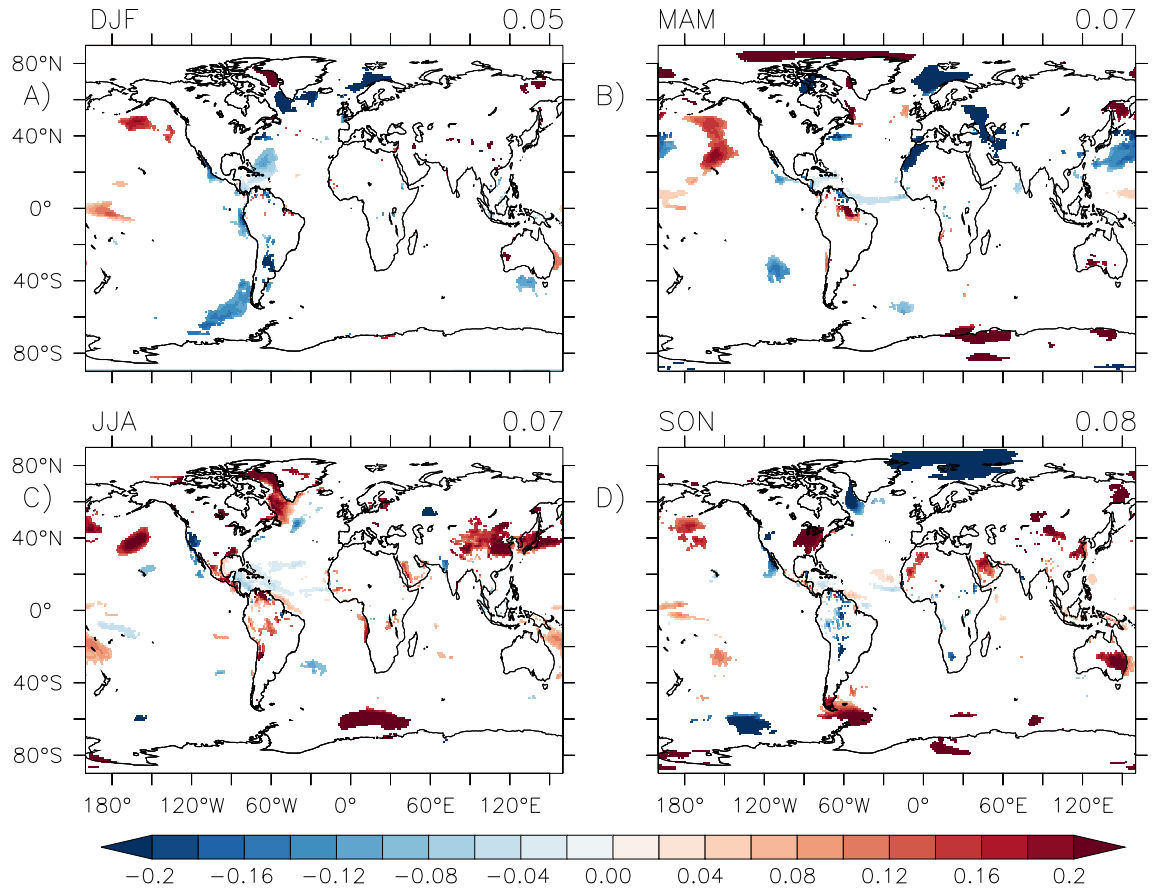


**Fig. 13** Seasonal Surface Air Temperature (tas)—Impact of increasing model resolution on modelled AMV response. Each panel shows the difference between the AMV High Resolution (HR) ensemble responses ($2AMV^{+}$-$2AMV^{-}$) and the Low Resolution (LR) responses. Regions where the difference is significant ($G_{er}$;$p < 0.05$) are shaded. A) Winter (Dec–Jan). B) Spring (Mar-May). C) Summer (Jun–Aug). D) Autumn (Sep–Nov). Units: C. Top right of each panel: fraction of the total number of gridpoints that are significant ($p < 0.05$)

model mean of $D_m$ is zero. This could arise because none of the $D_m$ are greater than zero (the AMV response does not change as resolution is increased), or a threshold ($R_c$) is spanned by a subset of the models ($m'$), but the resulting $D_{m'}$ are too small to be detected when meaned over all models.

Unlike in the previous sections, the significance of these results for resolution do appear to be somewhat sensitive to resampling (see SI section 1.3). Consequently, we only comment on the features that are robust to resampling in the following discussion. Additionally, we note that the *field significance* of many of these results is marginal.

Figures 13, 14 and 15 show that the impact of increasing model resolution is generally small; that is, we are unable to detect the impact of increased model resolution on the AMV response, although there are some regions where there are notable differences.

There are small significant changes in surface air temperature (tas) in the northern North Atlantic and Arctic in all seasons (Fig. 13), most notably in the Labrador Sea which sees colder (warmer) temperatures during DJF (JJA) at higher resolution, with a small cooling in the Barents Sea during MAM. These changes may arise due to resolution sensitivities in the mixed layer depth or sea ice, but could also arise from differences in the mean state of the sea ice cover in HR and LR controls—small differences in the mean sea ice extent could lead to large differences in the surface air temperature response between the resolutions. These changes are only marginally field significant, however.

The impact of resolution on the large scale circulation response is very weak and small compared to the mean response, with perhaps a slight positive mean sea level pressure response over southern South America in HR (Fig. 14 and SI section 1.3—Figure S8). But in none of the seasons are these results field significant.

The strongest impacts of increasing model resolution appears in the tropical precipitation response (Fig. 15). The AMV drives a northward displacement in the Atlantic ITCZ, represented by the dipole in Fig. 4. This northwards displacement is stronger in HR, resulting in a precipitation

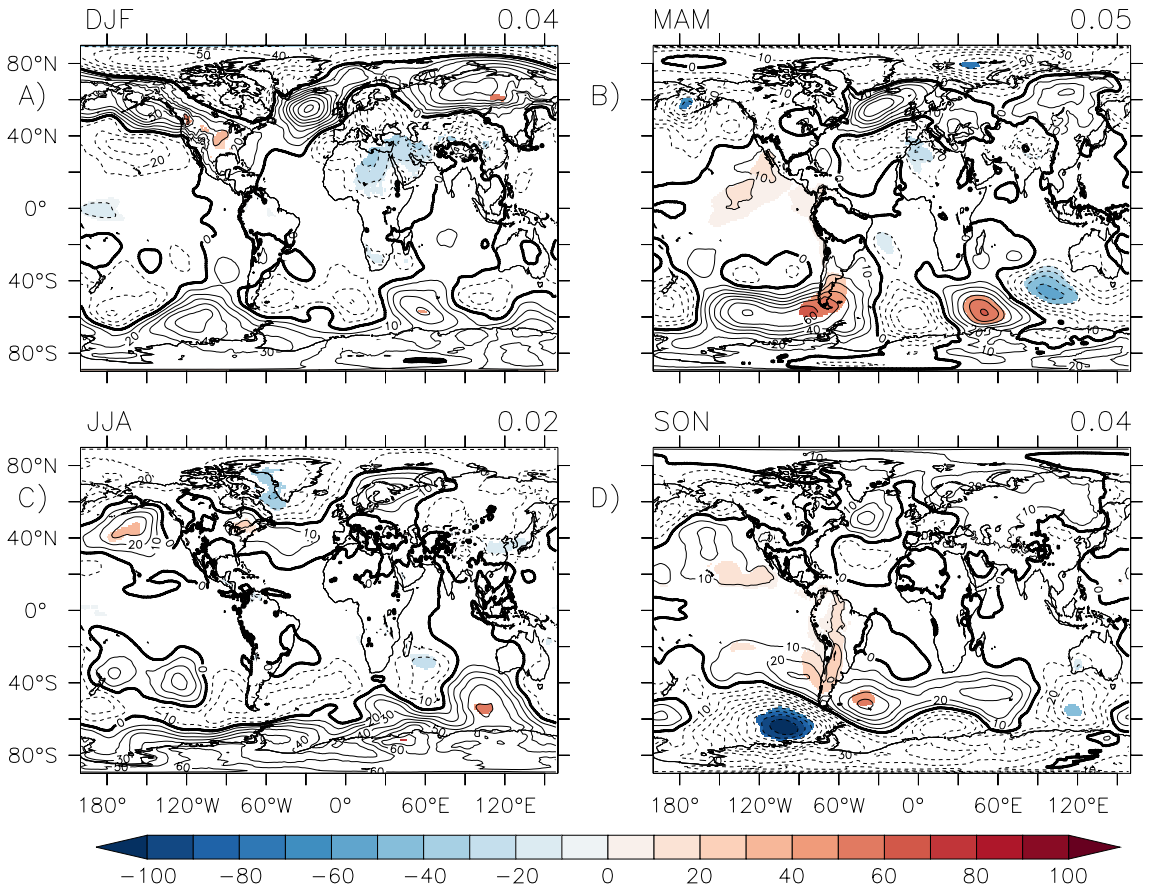


**Fig. 14** As Fig. 13, but for mean sea level pressure (psl). Units: Pa Contours are 20 Pa

*tripole* (difference between two displaced dipoles) in the Tropical Atlantic. This tripole is strongest in summer (JJA, Fig. 15c). This could arise due to an enhanced northern hemisphere warming response in the HR models during summer (Fig. 13c) (e.g. Frierson et al. 2013), which could drive a more northward shift in the ITCZ and the Hadley circulation.

There is also a small increase in precipitation over the west Pacific Ocean in winter and autumn (Fig. 15a, d), consistent with an enhanced ascent and a strengthening of the tropical Walker Circulation.

Because of the difficulty of distinguishing high and low resolution models across the ensemble, as discussed above, we can also examine the impact of resolution in individual models (see SI section 5—Figures S14–S28). This analysis shows that the models generally agree on the weak impacts seen across the full ensemble, but that the MPI-ESM 1.2 model shows a much stronger impact of resolution, with warmer temperatures over the wider Atlantic subpolar gyre, and a stronger Atlantic ITCZ displacement (SI section 5—Figures S18 and S28).

Despite this diversity, we have not been able to detect a large scale change in the climate response to the AMV after an increase of horizontal resolution (Figs. 2, 3, 4). Small consistent impacts of increased resolution are small regional variations in surface air temperature (tas) over the Arctic together with a northward shift in the ITCZ.

## 5 Discussion

The global scale climate response to the AMV in the multi-model multi-resolution ensemble mean (Figs. 2, 3, 4) is in broad agreement with the findings of previous coupled AMV experiments (Ruprich-Robert et al. 2017; Dong et al. 2006; Levine -et al. 2018). Key features of the surface air temperature, pressure and rainfall responses identified above are also seen in these studies. This similarity suggests that the pattern of the climate response to the AMV is broadly consistent across coupled climate models, but the details and the magnitudes of the model responses may differ (McGregor et al. 2018; Kajtar et al. 2018; Ruprich-Robert et al. 2021). This climate response is also broadly similar to that found in previous atmosphere-only AMV studies (Hodson et al. 2009; Sutton and Hodson 2007; Mohino et al. 2011; Davini et al. 2015; Peings and Magnusdottir 2014; Zhang and Delworth

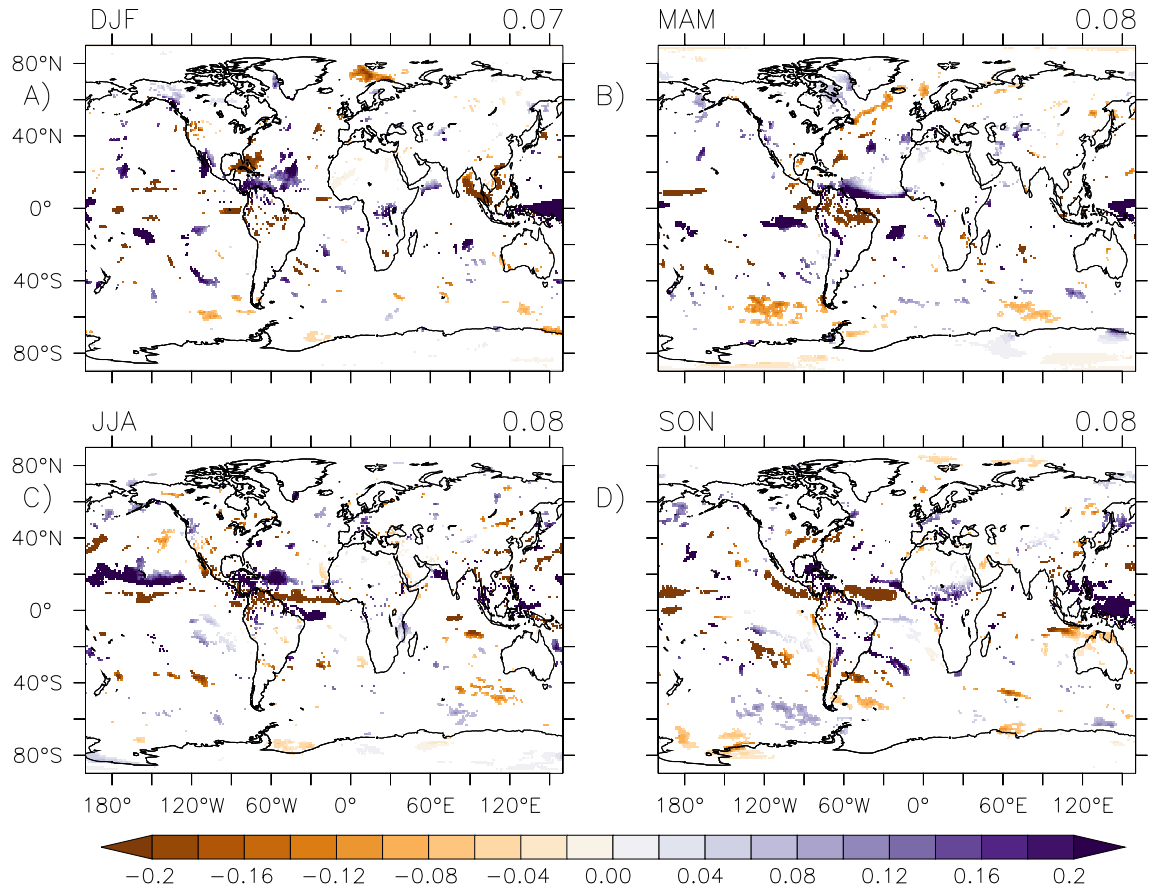


**Fig. 15** As Fig. 13, but for precipitation (pr). Units:mm/day

2006), however the response over the fixed-SST oceans in those experiments is generally weaker than seen in the coupled studies, suggesting that ocean-atmosphere coupling enhances the climate response to the AMV.

We have examined the difference between the $2AMV^{+}$ and $2AMV^{-}$ experiments, but does the climate respond differently to $2AMV^{+}$ and $2AMV^{-}$? In other words, how linear is the climate response to the AMV around the model climatology? We can examine this question by comparing both AMV responses to the model climatology (SI section 8—Figures S37–43). We conclude that the large-scale climate response is mostly linear—that is the $2 * AMV^{+} - Clim$ and $Clim - 2 * AMV^{-}$ responses have the same spatial structure as the $2 * AMV^{+} - 2 * AMV^{-}$ response (Figs. 2-4). We discuss this further in the SI (section 8).

Each model realization was integrated for 10 years. In our previous analysis we assumed that each of these years is statistically independent. If the climate response to the AMV forcing evolved over time (i.e. drifted), then this would be an incorrect assumption. To test this independence we can examine the influence of the *year* of the realization in a similar way to the influence of the models (Sect. 4.4—Figs. 9, 10), and ask the question: does this factor significantly affect the AMV response? Figures S44-S46 (SI section 9) demonstrate that there are only small regional impacts of this factor. In other words, the climate response to the AMV is largely constant across the 10 years of simulation (see SI section 9 for more details).

## 5.1 Comparison with observations

How does the modelled response to the AMV compare with estimates of the observed response? The observed climate evolved in response to multiple sources of forcings, not just the AMV, hence it is challenging to derived a robust estimate of the true observed response to the AMV. Previous observational studies have attempted this, and some show a similar European warming (Fig. 2) in observations (Gastineau and Frankignoul 2014; O'Reilly et al. 2017; Sutton and Dong 2012). The modelled circulation response (Fig. 3) is less consistent and does not show the negative NAO response seen in Gastineau and Frankignoul (2014) or Peings and Magnusdottir (2014). The pattern of the precipitation response (Fig. 4) is broadly consistent with the increase over Europe seen by O'Reilly et al. (2017) and Sutton and Dong (2012), and with the observed increases over the Sahel

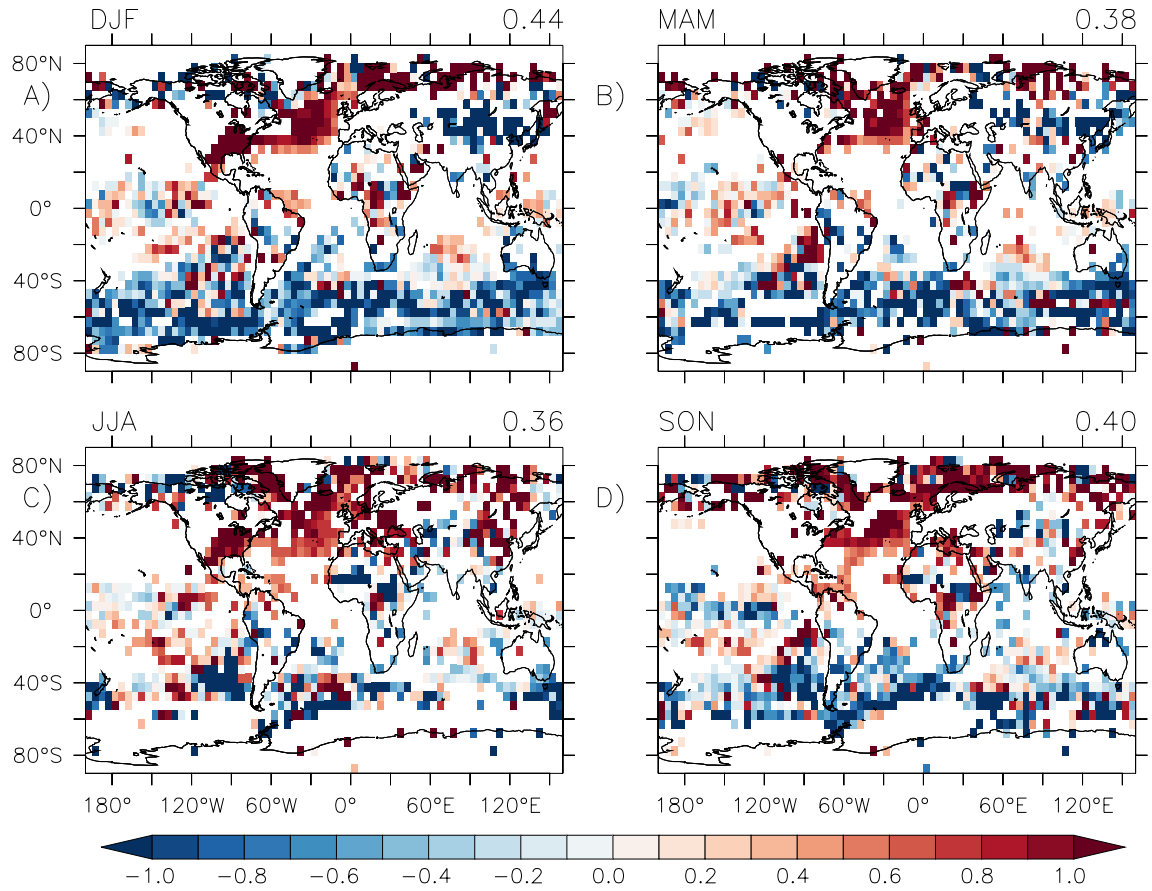


**Fig. 16** Scaled (x2) composite of observed surface air temperature (tas, HadCruT)—1930:1959 minus 1960:1989. The estimated forced trend has been removed from tas before computing the composite. Shaded regions are significant (two-sided t-test between the two time periods, $p < 0.05$). Units *K*. Top right of each panel: fraction of the total number of gridpoints that are significant ($p < 0.05$)

(Folland et al. 1986; Zhang and Delworth 2006), northeast Brazil (Uvo et al. 1998; Folland et al. 2001) and the reductions over North America (Sutton and Hodson 2005; Hodson et al. 2009).

Another approach to estimate the observed forced AMV response is to follow the method used to estimate the AMV forcing patterns (https://www.wcrp-climate.org/wgsip/documents/Tech-Note-1.pdf), by removing an estimate of the forced historical warming trend (from a historical forced multimodel ensemble mean—Figure 1a from Technical Note) from observed SSTs. Averaging the resulting residuals over the North Atlantic gives the (detrended) AMV index (Fig. 1b).

We can follow the same approach with any observed field: removing the estimate of the forced trend (from Technical Note Figure 1a, above) and considering the residuals as an AMV response. We can then form a composite difference from residuals between a high-AMV period (1930:1959) and a low-AMV period (1960:1959) (Fig. 1b). Figures 16 and 17 show these differences for surface air temperature (HadCRUT4—see Sect. 2.4.1) and mean sea level pressure (HadSLP2—see Sect. 2.4.1); the observed record of precipitation is too short for this approach. (We have multiplied these composites by 2 to aid comparison with the 2*AMV model responses previously shown.) An alternative approach is to composite based on when the AMV index (Fig. 1b) exceeds (falls below) plus (minus) one standard deviation. This approach produces similar results (SI section 7: Figures S35 and S36). Figures 16 and 2 show some consistencies between the modelled and estimated observed surface temperature response to the AMV: the warm anomaly of North America in DJF, extending to western Europe in JJA, and the cool Sahel anomaly band in JJA. Over the oceans, the cool Southern Ocean is consistent with the modelled response in most seasons, and the signal of eastern tropical Pacific cooling seen in the models is detectable in most seasons. The consistency is much lower for mean sea level pressure (psl) (Figs. 17 and 3). The greatest consistency appears in JJA, with a low pressure anomaly over North America, extending eastwards over the Atlantic to Europe. There is a hint of the modelled Aleutian high pressure response in DJF and JJA. Alternatively, we can examine the *amplitude* of the

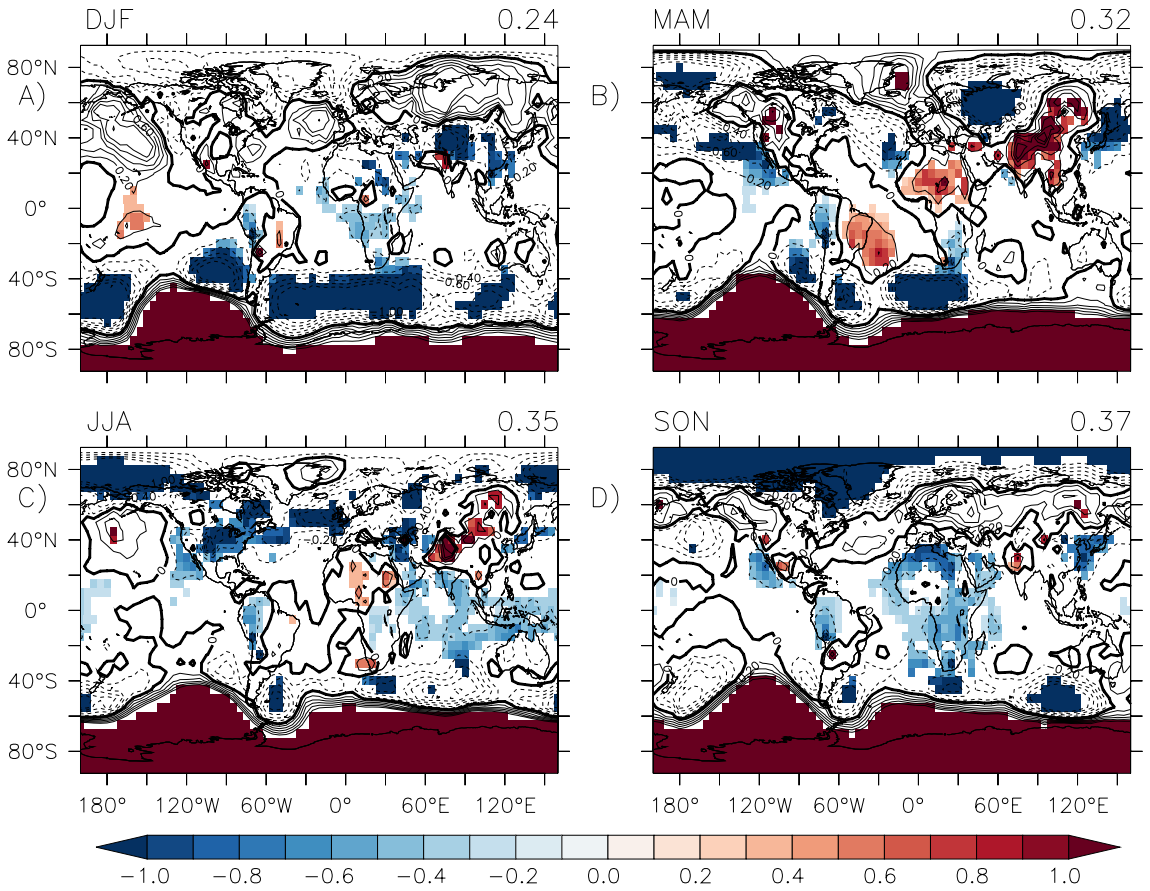


**Fig. 17** As Fig. 16, but for mean sea level pressure. Units: *Pa*

modelled AMV response compared to an observed estimate. This approach is motivated by the signal-to-noise paradox observed in seasonal forecasts; where the forecast amplitude of the North Atlantic Oscillation is about one-third of the observed amplitude (Scaife et al. 2014; Scaife and Smith 2018). If we project the observation residuals (i.e. detrended as above) onto the modelled response (Figs. 2 etc), we can estimate a timeseries ($\beta(t)$) of the observed response to the AMV for any variable (see SI section 7 for further details). If the real climate responds to the AMV with the same spatial pattern as the model, then $\beta(t)$ would match the AMV index exactly in both shape and amplitude. SI section 7—Figures S35 and S36 show that whilst the model responses do capture some of the multidecadal variability in the observations, this is somewhat weaker and out-of-phase with the observed AMV. The latter part of the observed record (1960 onwards) is generally much better captured. This suggests that the weaker response seen in the model, compared to observations, may be due to the greater uncertainties in the earlier part of the observational record. Overall, there is some evidence that the modelled response to the AMV is weaker than the observed response, but the limited observational data makes it hard to be definitive.

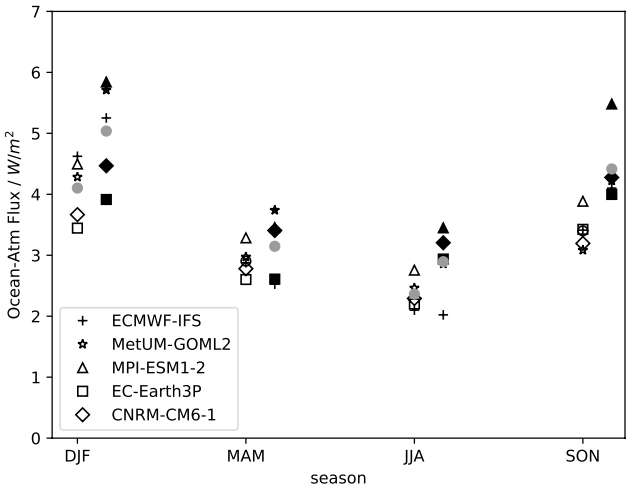


**Fig. 18** Comparison of (open symbols, left) upward surface latent heat fluxes ($2AMV^{+} - 2AMV^{-}$) and (black, right) net upward surface heat fluxes (latent, sensible, shortwave and longwave), both averaged over the AMV region (Fig. 1), for each season. Symbols show means over all ensemble members and resolutions for each model. Circle shows mean across all models. Grey filled circle denotes the model spread is significant from the ANOVA (e.g. $A_{em}$ in section 3 ( eqn. 3))

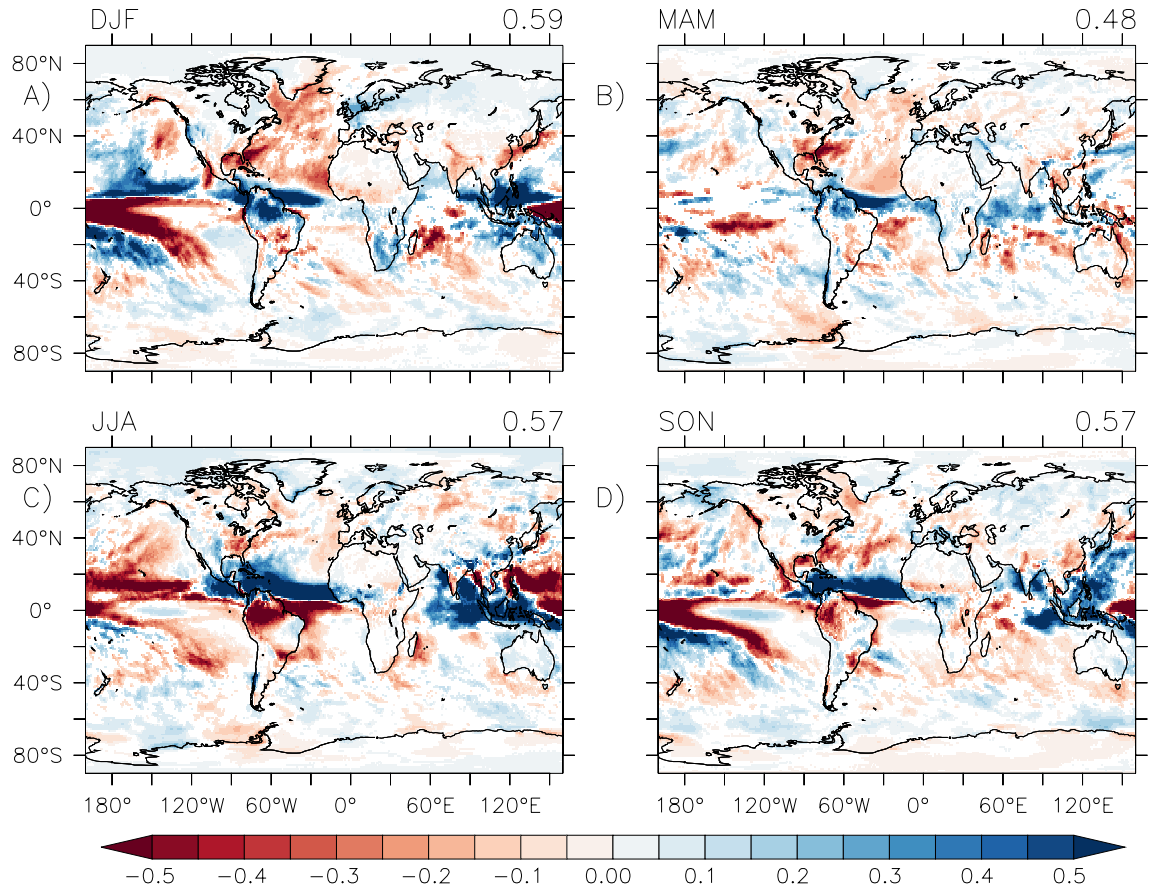


**Fig. 19** As Fig. 2, but for precipitation—evaporation. Units: *mm/day*

**Table 1** Atmosphere grid resolution in km for each model at low and high resolution configurations. The first number is the *nominal* resolution (derived from the model grid definition and threshold truncation (point 3) http://goo.gl/v1drZl (Appendix 2) or Klaver et al. (2020) supplementary) and the following number in brackets is the *effective* resolution (derived from the model grid's ability to resolve the KE spectra (see Klaver et al. 2020)

| Model | Low resolution | High resolution |
|---|---|---|
| CNRM-CM6-1 | 250 (≥625) | 100 (313) |
| EC-Earth | 100 (351) | 50 (238) |
| ECMWF-IFS | 100 (253) | 50 (185) |
| MetUM-GOML2 | 250 (≥625) | 100 (364) |
| MPIESM1.2 | 100 (364) | 50 (256) |

## 5.2 AMV forcing spread

Whilst the AMV SST anomalies are consistently maintained across models (Fig. 9, Figure S11), the resulting net ocean-atmosphere surface fluxes may differ across models. Examining this spread across models, the net surface latent heat fluxes released into the atmosphere over the North Atlantic AMV forcing region varies significantly across models in winter and summer, peaking in winter and autumn (Fig. 18). The spread increases when we consider the total net surface flux (Fig. 18). Hence, although the atmosphere in each model sees closely similar North Atlantic SST anomalies, there is a significant model spread in the resulting heat flux forcing of the atmosphere (perhaps due to a spread in conditions at the air–sea interface). This spread may arise from model formulation differences, or perhaps differences in the climatologies across the models (for example, the extent of sea ice cover over the Arctic). Such variation in forcing may be a significant factor in the model spread in the AMV climate response across models (Figs. 9-10). The model spread in surface air temperature (Fig. 9) over the Tropical Pacific appear to be partly related to this spread in AMV forcing (SI section 10—Figure S49) for part of the year. Ruprich-Robert et al. (2021) demonstrate that the latitude of the ITCZ varies across the model climatologies and that this explains a significant proportion of the spread in the Tropical Pacific response.

### 5.3 P–E

The AMV drives global changes in the hydrological cycle via changes in precipitation (Fig. 4). The AMV also drives changes in surface evaporation (Fig. 5). These changes result in the net surface moisture fluxes (p–e: precipitation–evaporation) (Fig. 19). Whilst the AMV drives a reduction in precipitation across the US in summer (Fig. 4c) the net impact on p-e is *positive* for the central and western US; due to a widespread reduction in surface evaporation (Fig. 5). In contrast, the AMV drives a strong seasonal cycle of p-e over northern South America; with increased downward moisture fluxes in DJF and net upward fluxes in JJA. The enhanced South Asian monsoon (Fig. 4c) results in a mixed net downward moisture flux, the increased rainfall being balanced somewhat by enhanced evaporation. Over Europe, there is notable seasonality, with increased downward moisture flux in winter, and a drier summer and autumn.

### 5.4 Summary

In broad agreement with other AMV impact studies (Sutton and Hodson 2005; Hodson et al. 2009; Dong et al. 2006; Ruprich-Robert et al. 2018; Levine -et al. 2018), we can summarize the global response to the AMV as a northward shift in tropical precipitation (hence a northward shift of the ITCZ and perhaps the Hadley cell) together with an adjustment in the tropical Walker circulation. The Hadley cell changes are likely driven by the hemispheric imbalance in heating (e.g. Kang et al. 2008) and lead to global changes in precipitation following the displacement of the ITCZ. Latent heat release over the Tropical Atlantic may then drive changes in the tropical Walker circulation as shown by Kucharski et al. (2011). The resultant surface wind changes over the Equatorial Pacific interact with the ocean driving enhanced upwelling, via a Bjerknes feedback, leading to a widespread eastern and central Pacific cooling (Li et al. 2016). This cooling increases subsidence and reduces convection over the East and Central Pacific, driving extratropical wavetrains (Scaife et al. 2017) leading to changes in extratropical circulation over the north Pacific and Atlantic. These large scale responses lead to widespread regional changes in temperature and circulation.

## 6 Conclusions

We have examined the global climate impact of the AMV in five coupled climate models, at two groups of atmospheric horizontal resolutions: low resolution (LR: 250–100 km) and high resolution (HR: 100–50 km) for each model. We have discussed the model mean climate response and where choice of model and resolution alters this response. Our key findings are:

- The AMV has a global-scale impact on climate, affecting global circulation, surface air temperature and rainfall. The positive AMV drives:
  - warming over much of Eurasia, northern Africa and North and South America (Fig. 2). This is accompanied by some regional cooling over land: Alaska, northern sub-Saharan Africa and India. These changes are partly due to the advection of warm (or cold) air, partly due to changing shortwave fluxes due to changes in cloud cover. Outside the Atlantic, the AMV drives widespread cold SSTs, most notably a PDO-like cooling over the Central and eastern Pacific. This cooling is likely driven by enhanced ocean upwelling.
  - a global shift in the hydrological cycle, characterized by a northward shift in the ITCZ over the Atlantic and Pacific and a displacement of the African Monsoon system, accompanied by reduced rainfall over the Tropical Pacific, and increased rainfall over Asia and the Maritime Continent (Fig. 4).
  - global-scale changes in circulation, characterized by ascent over the Atlantic and descent over the Pacific (Fig. 3). The response peaks in summertime (JJA), but there are significant impacts on the Aleutian low during winter (DJF) and spring (MAM)—these latter drive anomalous cooling over Alaska and western Canada in winter (DJF).

These findings are consistent with previous AMV experiments with atmosphere-only models (Sutton and Hodson 2005, 2007; Hodson et al. 2009; Davini et al. 2015; Vigaud et al. 2018; Omrani et al. 2014, 2016) and also more recent studies with coupled models (Ruprich-Robert et al. 2017, 2018; Levine -et al. 2018; Monerie et al. 2019).

- There is a global multimodel-mean AMV response across multiple variables ( $\alpha_e$—significant when compared to internal variability), but models disagree on the magnitude of this response in some regions ($A_{em}$)—most notably in the Tropics (Figs. 9 and 10). Part of this model variation may arise from the differing atmosphere heat flux forcings that result from the same SST pattern forcing pattern (Fig. 18).
- We are generally unable to detect a change in the multimodel mean responses as model resolution is increased, although the extent of the northward displacement of the ITCZ has some sensitivity to resolution (Fig. 15), moving further north at higher resolution. There is also some

evidence of an enhanced tropical Walker Circulation. This does not preclude the possibility that larger changes to the AMV response exist across a specific resolution threshold within our sample, or for resolutions greater than we have sampled here.

This study suggests that resolution (in the range we have sampled here) may not be a large source of uncertainty in experimental estimates of the large-scale impact of the AMV. Model variation is likely to be a more significant source of uncertainty. Resolution may play a greater role for smaller scale processes or extremes, such as hurricanes or temperature extremes. Future studies analysis will examine these impacts in these experiments. Given the widespread nature of the impacts of the AMV seen in this study, a better understanding of these model uncertainties, combined with good estimates of the future evolution of the AMV are crucial to predict near-term global climate changes. Further future analysis of the full CMIP6 DCPP-C AMV experiment ensemble will enhance our understanding and ability to do this.

## A Analysis of Variance (ANOVA)

In this section we outline the basis for Analysis of Variance (ANOVA) see Storch and Zwiers (1999, p117), Zwiers (1996) or Wilks (2019) for detailed explanations). ANOVA aims to decompose the total variance of a dataset into contributions from different factors. The significance of each contribution can then be assessed.

Consider a multi-model ensemble experiment with ($m = 1..M$) models and ($e = 1..E$) experiments, where each experiment was performed ($j = 1..J$) times.[1] Suppose we wish to examine the factors influencing Mean Sea Level Pressure (MSLP) in this ensemble. Assuming the models uses a common spatial grid, we can define MSLP at a grid point across all experiments ($e$), models ($m$) and ensemble members ($j$) to be $X_{emj}$. We can then express $X_{emj}$ as a linear combination of factors:

$$X_{emj} = \mu + \alpha_e + \beta_m + \gamma_{em} + \epsilon_{emj} \tag{5}$$

Here, $\mu$ is the average over all experiments, models and ensemble members:

$$\mu = \frac{1}{EMJ} \sum_{emj} X_{emj} \tag{6}$$

$\alpha_e$ is the part of MSLP that changes between experiment, but does **not** change between ensemble members or models. We could consider this the true experimental response (about which individual model responses will cluster). Because of the definition of $\mu$ (6), $\alpha_e$ is constrained to satisfy:

$$\sum_e \alpha_e = 0$$

$\beta_m$ is the part of MSLP that changes between models, but does **not** change between experiments or ensemble members. In other words, it is the model *bias* of a given model $m$. Again, $\beta_m$ is constrained in the same manner as $\alpha_e$:

$$\sum_m \beta_m = 0$$

$\gamma_{em}$ is often called the *interaction term*—it accounts for the across-experiment differences between the ensemble-means, once the model biases ($\beta_m$) have been accounted for. $\gamma_{em}$ is similarly constrained by the definitions of $\mu$, $\alpha_e$ and $\beta_m$ to satisfy:

$$\sum_e \gamma_{em} = \sum_m \gamma_{em} = 0$$

Finally, $\epsilon_{emj}$ describes the residual noise. $\epsilon_{emj}$ is assumed to be *independent* and *normally distributed* with a zero mean and a variance of $\sigma_\epsilon^2$, e.g. $\epsilon_{emj} \sim N(0, \sigma_\epsilon^2)$. Having proposed a linear statistical model for this variable, we can form hypotheses and construct tests. For example, is there a significant model bias between the models? In other words, do the models have a spread of MSLP climatologies that is detectable above the internal variability, $\epsilon_{emj}$? We can re-frame the question as: is $\sum_m \beta_m^2 > 0$?

To answer this question we first define the Total Sum of Squares, TSS

$$TSS = \sum_{emj} (X_{emj} - X_{\circ\circ\circ})^2$$

Where, $\circ$ implies a mean over that index—for example:

$$X_{\circ mj} = \frac{1}{E} \sum_e X_{emj}$$

On close inspection, as the noise term $\epsilon_{emj}$ is *independently distributed*, the cross terms between different $j$ vanish, hence $TSS$ can be decomposed as follows:

$$TSS = SS\alpha + SS\beta + SS\gamma + SS\epsilon \tag{7}$$

where

[1] The analysis can still be performed if the models have a different number of ensemble members, $j$, but the subsequent statistical tests will no longer be exact. See (See Storch and Zwiers 1999, p. 178).

$$SS\alpha = \sum_{emj} (X_{e\circ\circ} - X_{\circ\circ\circ})^2$$
$$SS\beta = \sum_{emj} (X_{\circ m\circ} - X_{\circ\circ\circ})^2$$
$$SS\gamma = \sum_{emj} (X_{em\circ} - X_{e\circ\circ} - X_{\circ m\circ} + X_{\circ\circ\circ})^2$$
$$SS\epsilon = \sum_{emj} (X_{emj} - X_{em\circ})^2$$

This is simply the familiar idea that the total variance is just the sum of individual sources of variance. We can then construct *unbiased estimators* of the terms on the right hand side of Eq. 5. Consequently, it can be shown (e.g. Storch and Zwiers 1999) that $SS\beta$ is an unbiased estimator of:

$$EJ \sum_m \beta_m^2 + (M-1)\sigma_\epsilon^2 \tag{8}$$

Similarly, it can be shown that $SS\epsilon$ is an unbiased estimator of

$$EM(J-1)\sigma_\epsilon^2 \tag{9}$$

Therefore the ratio

$$\frac{SS\beta/(M-1)}{SS\epsilon/EM(J-1)}$$

is an unbiased estimator of

$$\frac{\frac{EJ}{M-1}\sum_m \beta_m^2 + \sigma_\epsilon^2}{\sigma_\epsilon^2} \tag{10}$$

If $\sum_m \beta_m^2 > 0$ then this expression will be *greater* than 1. Formally we can then pose a null hypothesis $H_0$ and an alternative hypothesis $H_1$:

$$H_0 : \sum_m \beta_m^2 = 0$$
$$H_1 : \sum_m \beta_m^2 \neq 0$$

In other words, if at least one of $\beta_m$ is not equal to zero then we can reject the null hypothesis $H_0$. An F-test can be used to test $H_0$ by assessing whether the *F-statistic* (10) is *significantly* greater than 1 (using the F-distribution $F_{M-1,EM(J-1)}$). A significant result (e.g. $p < 0.05$) implies that the factor represented by $\beta_m$, in this case model bias, has a detectable effect on MSLP in this multi-model ensemble experiment. Comparing $\sum_m \beta_m^2$ to $\sigma_\epsilon^2$ in this way, allows us to assess whether the effects associated with $\beta_m$ are greater than the noise, $\epsilon_{emj}$. Similar estimators to (10), and hence similar tests, can be found for $\alpha_e$ and $\gamma_{em}$.

We can also estimate the size of the effect of a given factor on $X_{emj}$ in (5) by computing the *fraction of the variance explained* (FVE). Examination of (8) and (9) shows that:

$$SS\beta - \frac{M-1}{EM(J-1)} SS\epsilon = EJ \sum_m \beta_m^2$$

is an unbiased estimator of the variance of $\beta_m$.

Therefore:

$$FVE_\beta = \frac{SS\beta - \frac{M-1}{EM(J-1)} SS\epsilon}{TSS}$$

$FVE_\beta$ is (an unbiased estimate of) the fraction of the *total variance* (*TSS*), explained by $\beta_m$ (see 7). Similar expressions can also be found for $\alpha_e$ and $\gamma_{em}$.

Furthermore, it can be shown that ANOVA is a more general form of the t-test. For example, for the simpler case of one factor (e.g. one-way ANOVA) (5) becomes,

$$X_{mj} = \mu + \beta_m + \epsilon_{mj} \tag{11}$$

For the case of only two models (M=2—i.e. two samples) the F-statistic (10) for $\beta_m$ is exactly equal to the *square* of the corresponding two-sample t-statistic, and it can be shown (by integration) that the cumulative distributions of $t_n$ and $F_{1,n}$ are identical. Hence, one-way ANOVA with two *treatments* (M=2) is a two-sample t-test. Equally, we can extend this model to:

$$X_{mj} = \mu + \beta_m + C_j + \epsilon_{mj} \tag{12}$$

where $C_j$ is a factor that is the same for each $m$, but varies with ensemble member $j$. For $M = 2$, this reduces to a *paired* t-test—the presence of $C_j$ reduces the estimate of the noise variance ($\sigma_\epsilon^2$), which reduces the denominator in (10) leading to a larger F-statistic. A paired t-test similarly eliminates $C_j$ by computing pair differences between the two samples, which results in a reduced denominator in the corresponding t-statistic, and hence a more sensitive test. In both cases a source of variance is being removed to compare the remaining variance of interest with a better estimate of the noise.

We can extend the statistical model (5) to include more factors. In this paper, we consider consider the extra factor of *resolution*, and hence $X_{emrj}$, where $r$ is resolution. (5) can then be extended to include all possible interactions between these factors, and hence:

$$X_{emrj} = \mu + \alpha_e + \beta_m + \gamma_r + A_{em} + G_{er} + Z_{mr} + W_{emr} + \epsilon_{emrj} \tag{13}$$

Here, $A_{em}$ replaces $\gamma_{em}$. $\gamma_r$ represents the climatology changes that occur averaged across all models when resolution is changed, irrespective of the experiment. $G_{er}$ represents how the experimental response changes when resolution is changed—a key question for this paper. $Z_{mr}$ represents

how the spread of model climatologies changes when resolution is changed, irrespective of the experiment. $W_{emr}$ represents how the model spread between experiments changes when resolution is changed. In this way, we account for all possible sources of variance, which refines and reduces the estimate of the noise $\epsilon_{emrj}$, allowing us to detect smaller influences of the various factors than would otherwise be the case.

**Acknowledgements** The Authors would like to acknowledge the use of the UKRI funded JASMIN data analysis facility which was essential to the analysis and storage of PRIMAVERA project data. Ongoing curation of project data has been supported by the IS-ENES3 project that has received funding from the European Union' Horizon 2020 research and innovation programme under Grant Agreement No. 824084. Authors DH, PM, JS, PD, YRR, CDR acknowledge funding from the PRIMAVERA project (www.primavera-h2020.eu), funded by the European Union's Horizon 2020 programme under Grant Agreement 641727. PM was supported by U.K.–China Research and Innovation Partnership Fund through the Met Office Climate Science for Service Partnership (CSSP) China as part of the Newton Fund. PD thanks ECMWF for providing computing time in the framework of the special projects SPITDAVI. YRR was funded by the European Union's Horizon 2020 Research and Inovation Programme in the framework of the Marie Skłodowska-Curie grant INADEC (Grant Agreement 80015400). Author DH would like to thank Nick Klingaman and Linda Hirons for their extensive help with the MetUM-GOML model. This article was written with support (DH) from National Environmental Research Council (NERC) national capability grant for the North Atlantic Climate System: Integrated study (ACSIS) program (Grants NE/N018001/1, NE/N018044/1, NE/N018028/1, and NE/N018052/1). MMR is supported by a Juan de la Cierva Incorporacion research contract of MICINN (Spain). The authors wish to acknowledge use of the Ferret program for analysis and graphics in this paper. Ferret is a product of NOAA's Pacific Marine Environmental Laboratory. (Information is available at http://ferret.pmel.noaa.gov/Ferret/) and also the CF-python analysis package http://ncas-cms.github.io/cf-python/. Assembly of MetUM-GOML and development of MC-KPP was supported by the National Centre for Atmospheric Science and led by Dr. Nicholas Klingaman. The authors would also like to thank the three anonymous reviewers whose comments contributed to a much improved final manuscript.

**Funding** Funding was as set out in then Acknowledgements.

## Declarations

**Conflict of interest** The authors declare that they have no conflict of interest.

**Availability of data and code** The data and code used in this paper are available at https://doi.org/10.5281/zenodo.5884227.



## References

Allan R, Ansell T (2006) A new globally complete monthly historical Gridded Mean Sea Level Pressure Dataset (HadSLP2): 1850–2004. J Clim 19(22):5816–5842. https://doi.org/10.1175/jcli3937.1

Balsamo G, Beljaars A, Scipal K, Viterbo P, van den Hurk B, Hirschi M, Betts AK (2009) A revised hydrology for the ECMWF model: verification from field site to terrestrial water storage and impact in the integrated forecast system. J Hydrometeorol 10(3):623–643. https://doi.org/10.1175/2008JHM1068.1

Berckmans J, Woollings T, Demory ME, Vidale PL, Roberts M (2013) Atmospheric blocking in a high resolution climate model: influences of mean state, orography and eddy forcing. Atmos Sci Lett 14(1):34–40. https://doi.org/10.1002/asl2.412

Birkel SD, Mayewski PA, Maasch KA, Kurbatov AV, Lyon B (2018) Evidence for a volcanic underpinning of the Atlantic multidecadal oscillation. NPJ Clim Atmos Sci 1(1):1–7. https://doi.org/10.1038/s41612-018-0036-6. https://www.nature.com/articles/s41612-018-0036-6, number: 1 Publisher: Nature Publishing Group

Bjerknes J (1969) Atmospheric teleconnections from the equatorial pacific. Monthly Weather Rev 97(3):163–172. https://doi.org/10.1175/1520-0493(1969)097<0163:ATFTEP>2.3.CO;2. https://journals.ametsoc.org/view/journals/mwre/97/3/1520-0493_1969_097_0163_atftep_2_3_co_2.xml, publisher: American Meteorological Society Section: Monthly Weather Review

Boer GJ, Smith DM, Cassou C, Doblas-Reyes F, Danabasoglu G, Kirtman B, Kushnir Y, Kimoto M, Meehl GA, Msadek R, Mueller WA, Taylor KE, Zwiers F, Rixen M, Ruprich-Robert Y, Eade R (2016) The decadal climate prediction project (DCPP) contribution to CMIP6. Geosci Model Dev 9(10):3751–3777. https://doi.org/10.5194/gmd-9-3751-2016. https://www.geosci-model-dev.net/9/3751/2016/

Booth BBB, Dunstone NJ, Halloran PR, Andrews T, Bellouin N (2012) Aerosols implicated as a prime driver of twentieth-century North Atlantic climate variability. Nature 484(7393):228–232. https://doi.org/10.1038/nature10946

Bouillon S, Morales Maqueda MA, Legat V, Fichefet T (2009) An elastic-viscous-plastic sea ice model formulated on Arakawa B and C grids. Ocean Model 27(3):174–184. https://doi.org/10.1016/j.ocemod.2009.01.004. http://www.sciencedirect.com/science/article/pii/S1463500309000043

Buckley MW, Marshall J (2016) Observations, inferences, and mechanisms of the Atlantic Meridional Overturning Circulation: a review. Rev Geophys 54(1):5–63. https://doi.org/10.1002/2015RG000493

Cassou C, Terray L, Hurrell JW, Deser C (2004) North Atlantic Winter climate regimes: spatial asymmetry, stationarity with time, and oceanic forcing. J Clim 17(5):1055–1068. https://doi.org/10.1175/1520-0442(2004)017<3C1055:nawcrs>3E2.0.co;2

Christensen OB, Kjellström E (2020) Partitioning uncertainty components of mean climate and climate change in a large ensemble of European regional climate model projections. Clim Dyn 54(9):4293–4308. https://doi.org/10.1007/s00382-020-05229-y

Clement A, Bellomo K, Murphy LN, Cane MA, Mauritsen T, Rädel G, Stevens B (2015) The Atlantic Multidecadal Oscillation without a role for ocean circulation. Science 350(6258):320–324. https://doi.org/10.1126/science.aab3980. https://www.science.org/doi/

full/10.1126/science.aab3980, publisher: American Association for the Advancement of Science

Craig A, Valcke S, Coquart L (2017) Development and performance of a new version of the OASIS coupler, OASIS3-MCT_3.0. Geosci Model Dev 10(9):3297–3308. https://doi.org/10.5194/gmd-10-3297-2017. https://www.geosci-model-dev.net/10/3297/2017/

Czaja A, Frankignoul C, Minobe S, Vannière B (2019) Simulating the midlatitude atmospheric circulation: what might we gain from high-resolution modeling of air-sea interactions? Curr Clim Change Rep 5(4):390–406. https://doi.org/10.1007/s40641-019-00148-5

Davini P, Hardenberg J, Corti S (2015) Tropical origin for the impacts of the Atlantic Multidecadal Variability on the Euro-Atlantic climate. Environ Res Lett 10(9):094010. https://doi.org/10.1088/1748-9326/10/9/094010. publisher: IOP Publishing

Decharme B, Delire C, Minvielle M, Colin J, Vergnes JP, Alias A, Saint-Martin D, Séférian R, Sénési S, Voldoire A (2019) Recent changes in the ISBA-CTRIP land surface system for use in the CNRM-CM6 climate model and in global off-line hydrological applications. J Adv Model Earth Syst 11(5):1207–1252. https://doi.org/10.1029/2018MS001545

Delworth T, Manabe S, Stouffer RJ (1993) Interdecadal variations of the thermohaline circulation in a coupled ocean-atmosphere model. J Clim 6(11):1993–2011. https://doi.org/10.1175/1520-0442(1993)006<1993:IVOTTC>2.0.CO;2. https://journals.ametsoc.org/jcli/article/6/11/1993/36096/Interdecadal-Variations-of-the-Thermohaline, publisher: American Meteorological Society

Demory ME, Vidale PL, Roberts MJ, Berrisford P, Strachan J, Schiemann R, Mizielinski MS (2014) The role of horizontal resolution in simulating drivers of the global hydrological cycle. Clim Dyn 42(7):2201–2225. https://doi.org/10.1007/s00382-013-1924-4

Deser C, Alexander MA, Xie SP, Phillips AS (2010) Sea surface temperature variability: patterns and mechanisms. Ann Rev Mar Sci 2(1):115–143. https://doi.org/10.1146/annurev-marine-120408-151453

Dong B, Sutton RT (2007) Enhancement of ENSO Variability by a weakened Atlantic thermohaline circulation in a coupled GCM. J Clim 20(19):4920–4939. https://doi.org/10.1175/jcli4284.1

Dong B, Sutton RT, Scaife AA (2006) Multidecadal modulation of El Niño–Southern Oscillation (ENSO) variance by Atlantic Ocean sea surface temperatures. Geophys Res Lett 33(8). https://doi.org/10.1029/2006GL025766

Déqué M, Dreveton C, Braun A, Cariolle D (1994) The ARPEGE/IFS atmosphere model: a contribution to the French community climate modelling. Clim Dyn 10(4):249–266. https://doi.org/10.1007/BF00208992

Elsbury D, Peings Y, Saint-Martin D, Douville H, Magnusdottir G (2019) The atmospheric response to positive IPV, positive AMV, and their combination in boreal winter. J Clim 32(14):4193–4213. https://doi.org/10.1175/JCLI-D-18-0422.1. https://journals.ametsoc.org/jcli/article/32/14/4193/343959/The-Atmospheric-Response-to-Positive-IPV-Positive, publisher: American Meteorological Society

Enfield DB, Mestas-Nuñez AM, Trimble PJ (2001) The Atlantic multidecadal oscillation and its relation to rainfall and river flows in the continental U.S. Geophys Res Lett 28(10):2077–2080. https://doi.org/10.1029/2000GL012745

England MH, McGregor S, Spence P, Meehl GA, Timmermann A, Cai W, Gupta AS, McPhaden MJ, Purich A, Santoso A (2014) Recent intensification of wind-driven circulation in the Pacific and the ongoing warming hiatus. Nat Clim Chang 4(3):222–227. https://doi.org/10.1038/nclimate2106. https://www.nature.com/articles/nclimate2106, bandiera_abtest: a Cg_type: Nature Research Journals Number: 3 Primary_atype: Research Publisher: Nature Publishing Group Subject_term: Physical oceanography;Projection and prediction Subject_term_id: physical-oceanography;projection-and-prediction

Fichefet T, Maqueda MAM (1997) Sensitivity of a global sea ice model to the treatment of ice thermodynamics and dynamics. J Geophys Res Oceans 102(C6):12609–12646. https://doi.org/10.1029/97JC00480

Folland CK, Palmer TN, Parker DE (1986) Sahel rainfall and worldwide sea temperatures, 1901–85. Nature 320(6063):602–607. https://doi.org/10.1038/320602a0

Folland CK, Colman AW, Rowell DP, Davey MK (2001) Predictability of Northeast Brazil Rainfall and Real-Time Forecast Skill, 1987–98. Journal of Climate 14(9):1937–1958. https://doi.org/10.1175/1520-0442(2001)014%3C1937:ponbra%3E2.0.co;2

Fosser G, Khodayar S, Berg P (2015) Benefit of convection permitting climate model simulations in the representation of convective precipitation. Clim Dyn 44(1):45–60. https://doi.org/10.1007/s00382-014-2242-1

Frierson DMW, Hwang YT, Fučkar NS, Seager R, Kang SM, Donohoe A, Maroon EA, Liu X, Battisti DS (2013) Contribution of ocean overturning circulation to tropical rainfall peak in the Northern Hemisphere. Nat Geosci 6(11):940–944. https://doi.org/10.1038/ngeo1987. https://www.nature.com/articles/ngeo1987, number: 11 Publisher: Nature Publishing Group

Gastineau G, Frankignoul C (2014) Influence of the North Atlantic SST variability on the atmospheric circulation during the twentieth century. J Clim 28(4):1396–1416. https://doi.org/10.1175/jcli-d-14-00424.1

Gent PR, Mcwilliams JC (1990) Isopycnal mixing in ocean circulation models. J Phys Oceanogr 20(1):150–155. https://doi.org/10.1175/1520-0485(1990)020%3C0150:imiocm%3E2.0.co;2

Gill AE (1980) Some simple solutions for heat-induced tropical circulation. Q J R Meteorol Soc 106(449):447–462. https://doi.org/10.1002/qj.49710644905

Goldenberg SB, Landsea CW, Mestas-Nuñez AM, Gray WM (2001) The recent increase in atlantic hurricane activity: causes and implications. Science 293(5529):474–479. https://doi.org/10.1126/science.1060040

Haarsma R, Acosta M, Bakhshi R, Bretonnière PA, Caron LP, Castrillo M, Corti S, Davini P, Exarchou E, Fabiano F, Fladrich U, Fuentes Franco R, García-Serrano J, Hardenberg Jv, Koenigk T, Levine X, Meccia VL, Noije Tv, Oord Gvd, Palmeiro FM, Rodrigo M, Ruprich-Robert Y, Sager PL, Tourigny E, Wang S, Weele Mv, Wyser K (2020) HighResMIP versions of EC-Earth: EC-Earth3P and EC-Earth3P-HR – description, model computational performance and basic validation. Geosci Model Dev 13(8):3507–3527. https://doi.org/10.5194/gmd-13-3507-2020. https://gmd.copernicus.org/articles/13/3507/2020/. publisher: Copernicus GmbH

Hazeleger W, Bintanja R (2012) Studies with the EC-Earth seamless earth system prediction model. Clim Dyn 39(11):2609–2610. https://doi.org/10.1007/s00382-012-1577-8

He J, Kirtman B, Soden BJ, Vecchi GA, Zhang H, Winton M (2018) Impact of Ocean Eddy resolution on the sensitivity of precipitation to CO2 increase. Geophys Res Lett 45(14):7194–7203. https://doi.org/10.1029/2018GL078235

Hewitt HT, Roberts MJ, Hyder P, Graham T, Rae J, Belcher SE, Bourdallé-Badie R, Copsey D, Coward A, Guiavarch C, Harris C, Hill R, Hirschi JJM, Madec G, Mizielinski MS, Neininger E, New AL, Rioual JC, Sinha B, Storkey D, Shelly A, Thorpe L, Wood RA (2016) The impact of resolving the Rossby radius at mid-latitudes in the ocean: results from a high-resolution version of the Met Office GC2 coupled model. Geosci Model Dev 9(10):3655–3670. https://doi.org/10.5194/gmd-9-3655-2016. https://gmd.copernicus.org/articles/9/3655/2016/gmd-9-3655-2016.html, publisher: Copernicus GmbH

Hewitt HT, Bell MJ, Chassignet EP, Czaja A, Ferreira D, Griffies SM, Hyder P, McClean JL, New AL, Roberts MJ (2017) Will high-resolution global ocean models benefit coupled predictions on short-range to climate timescales? Ocean Model 120:120–136. https://doi.org/10.1016/j.ocemod.2017.11.002. https://www.sciencedirect.com/science/article/pii/S1463500317301774

Hirons LC, Klingaman NP, Woolnough SJ (2015) MetUM-GOML1: a near-globally coupled atmosphere–ocean-mixed-layer model. Geoscientific Model Development 8(2):363–379, https://doi.org/10.5194/gmd-8-363-2015. https://www.geosci-model-dev.net/8/363/2015/

Hodson DLR, Sutton RT (2008) Exploring multi-model atmospheric GCM ensembles with ANOVA. Clim Dyn 31(7):973–986. https://doi.org/10.1007/s00382-008-0372-z

Hodson DLR, Sutton RT (2012) The impact of resolution on the adjustment and decadal variability of the Atlantic meridional overturning circulation in a coupled climate model. Clim Dyn. https://doi.org/10.1007/s00382-012-1309-0

Hodson DLR, Sutton RT, Cassou C, Keenlyside N, Okumura Y, Zhou T (2009) Climate impacts of recent multidecadal changes in Atlantic Ocean Sea Surface Temperature: a multimodel comparison. Clim Dyn. https://doi.org/10.1007/s00382-009-0571-2

Hodson DLR, Robson JI, Sutton RT (2014) An Anatomy of the Cooling of the North Atlantic Ocean in the 1960s and 1970s. J Clim 27(21):8229–8243. https://doi.org/10.1175/JCLI-D-14-00301.1. https://journals.ametsoc.org/jcli/article/27/21/8229/33482/An-Anatomy-of-the-Cooling-of-the-North-Atlantic, publisher: American Meteorological Society

Hoerling M, Hurrell J, Eischeid J, Phillips A (2006) Detection and Attribution of Twentieth-Century Northern and Southern African Rainfall Change. J Clim 19(16):3989–4008. https://doi.org/10.1175/jcli3842.1

Huang B, Banzon VF, Freeman E, Lawrimore J, Liu W, Peterson TC, Smith TM, Thorne PW, Woodruff SD, Zhang HM (2015) Extended Reconstructed Sea Surface Temperature Version 4 (ERSST.v4). Part I: Upgrades and Intercomparisons. Journal of Climate 28(3):911–930, https://doi.org/10.1175/JCLI-D-14-00006.1, https://journals.ametsoc.org/jcli/article/28/3/911/106716/Extended-Reconstructed-Sea-Surface-Temperature, publisher: American Meteorological Society

Hurlburt HE, Metzger EJ, Hogan PJ, Tilburg CE, Shriver JF (2008) Steering of upper ocean currents and fronts by the topographically constrained abyssal circulation. Dynamics of Atmospheres and Oceans 45(3):102–134, https://doi.org/10.1016/j.dynatmoce.2008.06.003, https://www.sciencedirect.com/science/article/pii/S0377026508000328

Jackson LC, Roberts MJ, Hewitt HT, Iovino D, Koenigk T, Meccia VL, Roberts CD, Ruprich-Robert Y, Wood RA (2020) Impact of ocean resolution and mean state on the rate of AMOC weakening. Clim Dyn 55(7):1711–1732. https://doi.org/10.1007/s00382-020-05345-9, https://doi.org/10.1007/s00382-020-05345-9

Jung T, Miller MJ, Palmer TN, Towers P, Wedi N, Achuthavarier D, Adams JM, Altshuler EL, Cash BA, Kinter JL, Marx L, Stan C, Hodges KI (2012) High-Resolution Global Climate Simulations with the ECMWF Model in Project Athena: Experimental Design, Model Climate, and Seasonal Forecast Skill. J Clim 25(9):3155–3172. https://doi.org/10.1175/JCLI-D-11-00265.1. https://journals.ametsoc.org/view/journals/clim/25/9/jcli-d-11-00265.1.xml, publisher: American Meteorological Society Section: Journal of Climate

Jungclaus JH, Fischer N, Haak H, Lohmann K, Marotzke J, Matei D, Mikolajewicz U, Notz D, Storch JS (2013) Characteristics of the ocean simulations in the Max Planck Institute Ocean Model (MPIOM) the ocean component of the MPI-Earth system model. J Adv Model Earth Syst 5(2):422–446. https://doi.org/10.1002/jame.20023

Kajtar JB, Santoso A, McGregor S, England MH, Baillie Z (2018) Model under-representation of decadal Pacific trade wind trends and its link to tropical Atlantic bias. Clim Dyn 50(3):1471–1484. https://doi.org/10.1007/s00382-017-3699-5

Kang SM, Held IM, Frierson DMW, Zhao M (2008) The response of the ITCZ to extratropical thermal forcing: idealized slab-ocean experiments with a GCM. J Clim 21(14):3521–3532. https://doi.org/10.1175/2007jcli2146.1

Kerr RA (2000) A north atlantic climate pacemaker for the centuries. Science (New York, NY) 288(5473):1984–1985. https://doi.org/10.1126/science.288.5473.1984

Klaver R, Haarsma R, Vidale PL, Hazeleger W (2020) Effective resolution in high resolution global atmospheric models for climate studies. Atmos Sci Lett 21(4). https://doi.org/10.1002/asl.952

Knight JR, Folland CK, Scaife AA (2006) Climate impacts of the Atlantic Multidecadal Oscillation. Geophys Res Lett 33(17):L17706+. https://doi.org/10.1029/2006gl026242

Knutti R, Masson D, Gettelman A (2013) Climate model genealogy: generation CMIP5 and how we got there. Geophys Res Lett 40(6):1194–1199. https://doi.org/10.1002/grl.50256

Kucharski F, Kang IS, Farneti R, Feudale L (2011) Tropical Pacific response to 20th century Atlantic warming. Geophys Res Lett 38(3). https://doi.org/10.1029/2010GL046248

Kucharski F, Ikram F, Molteni F, Farneti R, Kang IS, No HH, King MP, Giuliani G, Mogensen K (2016) Atlantic forcing of Pacific decadal variability. Clim Dyn 46(7):2337–2351. https://doi.org/10.1007/s00382-015-2705-z

Kucharski F, Parvin A, Rodriguez-Fonseca B, Farneti R, Martin-Rey M, Polo I, Mohino E, Losada T, Mechoso CR (2016b) The Teleconnection of the Tropical Atlantic to Indo-Pacific Sea Surface Temperatures on Inter-Annual to Centennial Time Scales: a review of recent findings. Atmosphere 7(2):29. https://doi.org/10.3390/atmos7020029. https://www.mdpi.com/2073-4433/7/2/29, number: 2 Publisher: Multidisciplinary Digital Publishing Institute

Kwon YO, Seo H, Ummenhofer CC, Joyce TM (2020) Impact of multidecadal variability in Atlantic SST on winter atmospheric blocking. J Clim 33(3):867–892. https://doi.org/10.1175/JCLI-D-19-0324.1

Lean JL (2018) Estimating Solar Irradiance since 850 CE. Earth Space Sci 5(4):133–149. https://doi.org/10.1002/2017EA000357

Levine AFZ, Frierson DMW, McPhaden MJ (2018) AMO forcing of multidecadal pacific ITCZ variability. Journal of Clim 31(14):5749–5764, https://doi.org/10.1175/JCLI-D-17-0810.1. https://journals.ametsoc.org/jcli/article/31/14/5749/93377/AMO-Forcing-of-Multidecadal-Pacific-ITCZ, publisher: American Meteorological Society

Li X, Holland DM, Gerber EP, Yoo C (2014) Impacts of the north and tropical Atlantic Ocean on the Antarctic Peninsula and sea ice. Nature 505(7484):538–542, https://doi.org/10.1038/nature12945. https://www.nature.com/articles/nature12945, bandiera_abtest: a Cg_type: Nature Research Journals Number: 7484 Primary_atype: Research Publisher: Nature Publishing Group Subject_term: Atmospheric dynamics;Attribution;Climate and Earth system modelling;Projection and prediction Subject_term_id: atmospheric-dynamics;attribution;climate-and-earth-system-modelling;projection-and-prediction

Li X, Xie SP, Gille ST, Yoo C (2016) Atlantic-induced pan-tropical climate change over the past three decades. Nat Clim Chang 6(3):275–279. https://doi.org/10.1038/nclimate2840. https://www.nature.com/articles/nclimate2840, number: 3 Publisher: Nature Publishing Group

Livezey RE, Chen WY (1983) Statistical Field Significance and its Determination by Monte Carlo Techniques. Monthly Weather Rev 111(1):46–59. https://doi.org/10.1175/1520-0493(1983)111<0046:SFSAID>2.0.CO;2. https://journals.ametsoc.org/

view/journals/mwre/111/1/1520-0493_1983_111_0046_sfsaid_2_0_co_2.xml, publisher: American Meteorological Society Section: Monthly Weather Review

Lyu K, Yu JY (2017) Climate impacts of the Atlantic Multidecadal Oscillation simulated in the CMIP5 models: A re-evaluation based on a revised index. Geophys Res Lett 44(8):3867–3876. https://doi.org/10.1002/2017GL072681

Lyu K, Yu JY, Paek H (2017) The Influences of the Atlantic Multidecadal Oscillation on the Mean Strength of the North Pacific subtropical high during boreal winter. J Clim 30(1):411–426. https://doi.org/10.1175/JCLI-D-16-0525.1. https://journals.ametsoc.org/view/journals/clim/30/1/jcli-d-16-0525.1.xml, publisher: American Meteorological Society Section: Journal of Climate

Madec G, Bourdallé-Badie R, Bouttier PA, Bricaud C, Bruciaferri D, Calvert D, Chanut J, Clementi E, Coward A, Delrosso D, Ethé C, Flavoni S, Graham T, Harle J, Iovino D, Lea D, Lévy C, Lovato T, Martin N, Masson S, Mocavero S, Paul J, Rousset C, Storkey D, Storto A, Vancoppenolle M (2017) NEMO ocean engine. https://doi.org/10.5281/zenodo.1472492. https://zenodo.org/record/1472492#.XkPvkeGnzRY

Marzocchi A, Hirschi JJM, Holliday NP, Cunningham SA, Blaker AT, Coward AC (2015) The North Atlantic subpolar circulation in an eddy-resolving global ocean model. J Mar Syst 142:126–143. https://doi.org/10.1016/j.jmarsys.2014.10.007. https://www.sciencedirect.com/science/article/pii/S0924796314002437

Masson V, Moigne PL, Martin E, Faroux S, Alias A, Alkama R, Belamari S, Barbu A, Boone A, Bouyssel F, Brousseau P, Brun E, Calvet JC, Carrer D, Decharme B, Delire C, Donier S, Essaouini K, Gibelin AL, Giordani H, Habets F, Jidane M, Kerdraon G, Kourzeneva E, Lafaysse M, Lafont S, Lebeaupin Brossier C, Lemonsu A, Mahfouf JF, Marguinaud P, Mokhtari M, Morin S, Pigeon G, Salgado R, Seity Y, Taillefer F, Tanguy G, Tulet P, Vincendon B, Vionnet V, Voldoire A (2013) The SURFEXv7.2 land and ocean surface platform for coupled or offline simulation of earth surface variables and fluxes. Geosci Model Dev 6(4):929–960. https://doi.org/10.5194/gmd-6-929-2013. https://www.geosci-model-dev.net/6/929/2013/gmd-6-929-2013.html

McGregor S, Timmermann A, Stuecker MF, England MH, Merrifield M, Jin FF, Chikamoto Y (2014) Recent Walker circulation strengthening and Pacific cooling amplified by Atlantic warming. Nature Climate Change 4(10):888–892, https://doi.org/10.1038/nclimate2330, https://www.nature.com/articles/nclimate2330, number: 10 Publisher: Nature Publishing Group

McGregor S, Stuecker MF, Kajtar JB, England MH, Collins M (2018) Model tropical Atlantic biases underpin diminished Pacific decadal variability. Nature Climate Change 8(6):493–498, https://doi.org/10.1038/s41558-018-0163-4, https://www.nature.com/articles/s41558-018-0163-4, number: 6 Publisher: Nature Publishing Group

Meehl GA, Hu A, Castruccio F, England MH, Bates SC, Danabasoglu G, McGregor S, Arblaster JM, Xie SP, Rosenbloom N (2021) Atlantic and Pacific tropics connected by mutually interactive decadal-timescale processes. Nat Geosci 14(1):36–42. https://doi.org/10.1038/s41561-020-00669-x. https://www.nature.com/articles/s41561-020-00669-x, number: 1 Publisher: Nature Publishing Group

Minobe S, Kuwano-Yoshida A, Komori N, Xie SP, Small RJ (2008) Influence of the Gulf Stream on the troposphere. Nature 452(7184):206–209. https://doi.org/10.1038/nature06690. https://www.nature.com/articles/nature06690, bandiera_abtest: a Cg_type: Nature Research Journals Number: 7184 Primary_atype: Research Publisher: Nature Publishing Group

Mohino E, Janicot S, Bader J (2011) Sahel rainfall and decadal to multi-decadal sea surface temperature variability. Clim Dyn 37(3):419–440. https://doi.org/10.1007/s00382-010-0867-2

Monerie PA, Robson J, Dong B, Hodson DLR, Klingaman NP (2019) Effect of the Atlantic multidecadal variability on the global monsoon. Geophys Res Lett 46(3):1765–1775. https://doi.org/10.1029/2018GL080903

Monerie PA, Robson J, Dong B, Hodson D (2020) Role of the Atlantic multidecadal variability in modulating East Asian climate. Clim Dyn. https://doi.org/10.1007/s00382-020-05477-y

Montégut CdB, Madec G, Fischer AS, Lazar A, Iudicone D (2004) Mixed layer depth over the global ocean: an examination of profile data and a profile-based climatology. J Geophys Res Oceans 109(C12). https://doi.org/10.1029/2004JC002378

Morice CP, Kennedy JJ, Rayner NA, Jones PD (2012) Quantifying uncertainties in global and regional temperature change using an ensemble of observational estimates: the HadCRUT4 data set. J Geophys Res Atmos 117(D8). https://doi.org/10.1029/2011JD017187

Nigam S, Ruiz-Barradas A, Chafik L (2018) Gulf Stream Excursions and Sectional Detachments Generate the Decadal Pulses in the Atlantic Multidecadal Oscillation. J Clim 31(7):2853–2870. https://doi.org/10.1175/JCLI-D-17-0010.1. https://journals.ametsoc.org/view/journals/clim/31/7/jcli-d-17-0010.1.xml, publisher: American Meteorological Society Section: Journal of Climate

Noilhan J, Planton S (1989) A Simple Parameterization of Land Surface Processes for Meteorological Models. Monthly Weather Rev 117(3):536–549. https://doi.org/10.1175/1520-0493(1989)117<0536:ASPOLS>2.0.CO;2

Omrani NE, Keenlyside NS, Bader J, Manzini E (2014) Stratosphere key for wintertime atmospheric response to warm Atlantic decadal conditions. '//' 42(3–4):649–663. https://doi.org/10.1007/s00382-013-1860-3

Omrani NE, Bader J, Keenlyside NS, Manzini E (2016) Troposphere-stratosphere response to large-scale North Atlantic Ocean variability in an atmosphere/ocean coupled model. Clim Dyn 46(5):1397–1415. https://doi.org/10.1007/s00382-015-2654-6

Otterå OH, Bentsen M, Drange H, Suo L (2010) External forcing as a metronome for Atlantic multidecadal variability. Nat Geosci 3(10):688–694. https://doi.org/10.1038/ngeo955. https://www.nature.com/articles/ngeo955

O'Reilly CH, Woollings T, Zanna L (2017) The dynamical influence of the Atlantic multidecadal oscillation on continental climate. J Clim 30(18):7213–7230. https://doi.org/10.1175/JCLI-D-16-0345.1

Parfitt R, Czaja A, Minobe S, Kuwano-Yoshida A (2016) The atmospheric frontal response to SST perturbations in the Gulf Stream region. Geophys Res Lett 43(5):2299–2306. https://doi.org/10.1002/2016GL067723

Peings Y, Magnusdottir G (2014) Forcing of the wintertime atmospheric circulation by the multidecadal fluctuations of the North Atlantic ocean. Environ Res Lett 9(3):034018. https://doi.org/10.1088/1748-9326/9/3/034018

Qasmi S, Cassou C, Boé J (2017) Teleconnection between Atlantic multidecadal variability and European temperature: diversity and evaluation of the coupled model intercomparison project phase 5 models. Geophys Res Lett 44(21):11,140-11,149. https://doi.org/10.1002/2017GL074886

Roberts CD, Senan R, Molteni F, Boussetta S, Mayer M, Keeley SPE (2018) Climate model configurations of the ECMWF Integrated Forecasting System (ECMWF-IFS cycle 43r1) for HighResMIP. Geosci Model Dev 11(9):3681–3712. https://doi.org/10.5194/gmd-11-3681-2018

Rodríguez-Fonseca B, Polo I, García-Serrano J, Losada T, Mohino E, Mechoso CR, Kucharski F (2009) Are Atlantic Niños enhancing Pacific ENSO events in recent decades? Geophys Res Lett 36(20). https://doi.org/10.1029/2009GL040048

Ruggieri P, Bellucci A, Nicolí D, Athanasiadis PJ, Gualdi S, Cassou C, Castruccio F, Danabasoglu G, Davini P, Dunstone N, Eade

R, Gastineau G, Harvey B, Hermanson L, Qasmi S, Ruprich-Robert Y, Sanchez-Gomez E, Smith D, Wild S, Zampieri M (2021) Atlantic Multidecadal Variability and North Atlantic Jet: A Multimodel View from the Decadal Climate Prediction Project. Journal of Climate 34(1):347–360, https://doi.org/10.1175/JCLI-D-19-0981.1, https://journals.ametsoc.org/view/journals/clim/34/1/JCLI-D-19-0981.1.xml, publisher: American Meteorological Society Section: Journal of Climate

Ruprich-Robert Y, Cassou C (2015) Combined influences of seasonal East Atlantic Pattern and North Atlantic Oscillation to excite Atlantic multidecadal variability in a climate model. Clim Dyn 44(1):229–253. https://doi.org/10.1007/s00382-014-2176-7

Ruprich-Robert Y, Msadek R, Castruccio F, Yeager S, Delworth T, Danabasoglu G (2017) Assessing the Climate Impacts of the Observed Atlantic Multidecadal Variability Using the GFDL CM2.1 and NCAR CESM1 Global Coupled Models. Journal of Climate 30(8):2785–2810, https://doi.org/10.1175/JCLI-D-16-0127.1, https://journals.ametsoc.org/jcli/article/30/8/2785/95114/Assessing-the-Climate-Impacts-of-the-Observed, publisher: American Meteorological Society

Ruprich-Robert Y, Delworth T, Msadek R, Castruccio F, Yeager S, Danabasoglu G (2018) Impacts of the Atlantic Multidecadal Variability on North American Summer Climate and Heat Waves. Journal of Climate 31(9):3679–3700, https://doi.org/10.1175/JCLI-D-17-0270.1, https://journals.ametsoc.org/jcli/article/31/9/3679/89307/Impacts-of-the-Atlantic-Multidecadal-Variability, publisher: American Meteorological Society

Ruprich-Robert Y, Moreno-Chamarro E, Levine X, Bellucci A, Cassou C, Castruccio F, Davini P, Eade R, Gastineau G, Hermanson L, Hodson D, Lohmann K, Lopez-Parages J, Monerie PA, Nicolì D, Qasmi S, Roberts CD, Sanchez-Gomez E, Danabasoglu G, Dunstone N, Martin-Rey M, Msadek R, Robson J, Smith D, Tourigny E (2021) Impacts of Atlantic multidecadal variability on the tropical Pacific: a multi-model study. npj Climate and Atmospheric Science 4(1):1–11, https://doi.org/10.1038/s41612-021-00188-5, https://www.nature.com/articles/s41612-021-00188-5, number: 1 Publisher: Nature Publishing Group

Salas Mélia D (2002) A global coupled sea ice-ocean model. Ocean Modelling 4(2):137–172, https://doi.org/10.1016/S1463-5003(01)00015-4, http://www.sciencedirect.com/science/article/pii/S1463500301000154

Sato M, Hansen JE, McCormick MP, Pollack JB (1993) Stratospheric aerosol optical depths, 1850–1990. J Geophys Res 98(D12):22987–22994. https://doi.org/10.1029/93jd02553

Scaife AA, Smith D (2018) A signal-to-noise paradox in climate science. npj Climate and Atmospheric Science 1(1), https://doi.org/10.1038/s41612-018-0038-4

Scaife AA, Arribas A, Blockley E, Brookshaw A, Clark RT, Dunstone N, Eade R, Fereday D, Folland CK, Gordon M, Hermanson L, Knight JR, Lea DJ, MacLachlan C, Maidens A, Martin M, Peterson AK, Smith D, Vellinga M, Wallace E, Waters J, Williams A (2014) Skillful long-range prediction of European and North American winters. Geophys Res Lett 41(7):2014GL059637-2519. https://doi.org/10.1002/2014gl059637

Scaife AA, Comer RE, Dunstone NJ, Knight JR, Smith DM, MacLachlan C, Martin N, Peterson KA, Rowlands D, Carroll EB, Belcher S, Slingo J (2017) Tropical rainfall, Rossby waves and regional winter climate predictions. Q J R Meteorol Soc 143(702):1–11. https://doi.org/10.1002/qj.2910

Schiemann R, Demory ME, Shaffrey LC, Strachan J, Vidale PL, Mizielinski MS, Roberts MJ, Matsueda M, Wehner MF, Jung T (2017) The Resolution Sensitivity of Northern Hemisphere Blocking in Four 25-km Atmospheric Global Circulation Models. Journal of Climate 30(1):337–358, https://doi.org/10.1175/JCLI-D-16-0100.1, https://journals.ametsoc.org/view/journals/clim/30/1/jcli-d-16-0100.1.xml, publisher: American Meteorological Society Section: Journal of Climate

Shapiro LJ, Goldenberg SB (1998) Atlantic Sea Surface Temperatures and Tropical Cyclone Formation. Journal of Climate 11(4):578–590. https://doi.org/10.1175/1520-0442(1998)011%3C0578:asstat%3E2.0.co;2

Smith DM, Murphy JM (2007) An objective ocean temperature and salinity analysis using covariances from a global climate model. J Geophys Res 112(C2):C02022+. https://doi.org/10.1029/2005jc003172

Stevens B, Giorgetta M, Esch M, Mauritsen T, Crueger T, Rast S, Salzmann M, Schmidt H, Bader J, Block K, Brokopf R, Fast I, Kinne S, Kornblueh L, Lohmann U, Pincus R, Reichler T, Roeckner E (2013) Atmospheric component of the MPI-M Earth System Model: ECHAM6. Journal of Advances in Modeling Earth Systems 5(2):146–172. https://doi.org/10.1002/jame.20015

Storch Hv, Zwiers FW (1999) Statistical Analysis in Climate Research. Cambridge University Press, Cambridge, https://doi.org/10.1017/CBO9780511612336, https://www.cambridge.org/core/books/statistical-analysis-in-climate-research/9125090F106D2845485E4BACD79B9695

Sun C, Li J, Zhao S (2015) Remote influence of Atlantic multidecadal variability on Siberian warm season precipitation. Scientific Reports 5(1):16853, https://doi.org/10.1038/srep16853, https://www.nature.com/articles/srep16853, bandiera_abtest: a Cc_license_type: cc_by Cg_type: Nature Research Journals Number: 1 Primary_atype: Research Publisher: Nature Publishing Group Subject_term: Atmospheric dynamics;Climate change;Hydrology;Planetary science Subject_term_id: atmospheric-dynamics;climate-change;hydrology;planetary-science

Sutton RT, Dong B (2012) Atlantic Ocean influence on a shift in European climate in the 1990s. Nature Geoscience 5(11):788–792, https://doi.org/10.1038/ngeo1595, https://www.nature.com/articles/ngeo1595

Sutton RT, Hodson DLR (2005) Atlantic Ocean Forcing of North American and European Summer Climate. Science 309(5731):115–118. https://doi.org/10.1126/science.1109496

Sutton RT, Hodson DLR (2007) Climate Response to Basin-Scale Warming and Cooling of the North Atlantic Ocean. J Clim 20(5):891–907. https://doi.org/10.1175/jcli4038.1

Swingedouw D, Ortega P, Mignot J, Guilyardi E, Masson-Delmotte V, Butler PG, Khodri M, Séférian R (2015) Bidecadal North Atlantic ocean circulation variability controlled by timing of volcanic eruptions. Nature Communications 6(1):6545, https://doi.org/10.1038/ncomms7545, https://www.nature.com/articles/ncomms7545, bandiera_abtest: a Cg_type: Nature Research Journals Number: 1 Primary_atype: Research Publisher: Nature Publishing Group Subject_term: Atmospheric science;Climate-change impacts;Palaeoceanography;Volcanology Subject_term_id: atmospheric-science;climate-change-impacts;palaeoceanography;volcanology

Ting M, Kushnir Y, Seager R, Li C (2011) Robust features of Atlantic multi-decadal variability and its climate impacts. Geophys Res Lett 38(17):L17705+. https://doi.org/10.1029/2011gl048712

Undorf S, Bollasina MA, Booth BBB, Hegerl GC (2018) Contrasting the Effects of the 1850-1975 Increase in Sulphate Aerosols from North America and Europe on the Atlantic in the CESM. Geophys Res Lett 45(21):11,930-11,940. https://doi.org/10.1029/2018GL079970

Uvo CB, Repelli CA, Zebiak SE, Kushnir Y (1998) The Relationships between Tropical Pacific and Atlantic SST and Northeast Brazil Monthly Precipitation. Journal of Climate 11(4):551–562. https://doi.org/10.1175/1520-0442(1998)011%3C0551:trbtpa%3E2.0.co;2

Valcke S (2013) The OASIS3 coupler: a European climate modelling community software. Geoscientific Model Development

6(2):373–388, https://doi.org/10.5194/gmd-6-373-2013, https://www.geosci-model-dev.net/6/373/2013/

Vancoppenolle M, Bouillon S, Fichefet T, Goosse H, Arzel O, Morales Maqueda MA, Madec G (2012) LIM The Louvain-la-Neuve sea Ice Model. http://www.climate.be/users/lecomte/LIM3_users_guide_2012.pdf

Vellinga M, Wood RA (2002) Global Climatic Impacts of a Collapse of the Atlantic Thermohaline Circulation. Clim Change 54(3):251–267. https://doi.org/10.1023/a:1016168827653

Vigaud N, Ting M, Lee DE, Barnston AG, Kushnir Y (2018) Multiscale Variability in North American Summer Maximum Temperatures and Modulations from the North Atlantic Simulated by an AGCM. Journal of Climate 31(7):2549–2562, https://doi.org/10.1175/JCLI-D-17-0392.1, https://journals.ametsoc.org/jcli/article/31/7/2549/89965/Multiscale-Variability-in-North-American-Summer, publisher: American Meteorological Society

Voldoire A, Saint-Martin D, Sénési S, Decharme B, Alias A, Chevallier M, Colin J, Guérémy JF, Michou M, Moine MP, Nabat P, Roehrig R, Mélia DSy, Séférian R, Valcke S, Beau I, Belamari S, Berthet S, Cassou C, Cattiaux J, Deshayes J, Douville H, Ethé C, Franchistéguy L, Geoffroy O, Lévy C, Madec G, Meurdesoif Y, Msadek R, Ribes A, Sanchez-Gomez E, Terray L, Waldman R, (2019) Evaluation of CMIP6 DECK Experiments With CNRM-CM6-1. Journal of Advances in Modeling Earth Systems 11(7):2177–2213. https://doi.org/10.1029/2019MS001683

Wallace JM, Gutzler DS (1981) Teleconnections in the Geopotential Height Field during the Northern Hemisphere Winter. Monthly Weather Review 109(4):784–812, https://doi.org/10.1175/1520-0493(1981)109<0784:TITGHF>2.0.CO;2, https://journals.ametsoc.org/view/journals/mwre/109/4/1520-0493_1981_109_0784_titghf_2_0_co_2.xml, publisher: American Meteorological Society Section: Monthly Weather Review

Walters D, Boutle I, Brooks M, Melvin T, Stratton R, Vosper S, Wells H, Williams K, Wood N, Allen T, Bushell A, Copsey D, Earnshaw P, Edwards J, Gross M, Hardiman S, Harris C, Heming J, Klingaman N, Levine R, Manners J, Martin G, Milton S, Mittermaier M, Morcrette C, Riddick T, Roberts M, Sanchez C, Selwood P, Stirling A, Smith C, Suri D, Tennant W, Vidale PL, Wilkinson J, Willett M, Woolnough S, Xavier P (2017) The Met Office Unified Model Global Atmosphere 6.0/6.1 and JULES Global Land 6.0/6.1 configurations. Geoscientific Model Development 10(4):1487–1520, https://doi.org/10.5194/gmd-10-1487-2017, https://www.geosci-model-dev.net/10/1487/2017/

Wang C (2018) A review of ENSO theories. Natl Sci Rev 5(6):813–825. https://doi.org/10.1093/nsr/nwy104

Watanabe M, Tatebe H (2019) Reconciling roles of sulphate aerosol forcing and internal variability in Atlantic multidecadal climate changes. Clim Dyn 53(7):4651–4665. https://doi.org/10.1007/s00382-019-04811-3

Wilks DS (2019) Chapter 5—Frequentist Statistical Inference. In: Wilks DS (ed) Statistical Methods in the Atmospheric Sciences (Fourth Edition), Elsevier, pp 143–207, https://doi.org/10.1016/B978-0-12-815823-4.00005-5, https://www.sciencedirect.com/science/article/pii/B9780128158234000055

Yip S, Ferro CAT, Stephenson DB, Hawkins E (2011) A Simple, Coherent Framework for Partitioning Uncertainty in Climate Predictions. J Clim 24(17):4634–4643. https://doi.org/10.1175/2011JCLI4085.1

Zhang L, Delworth TL (2015) Analysis of the Characteristics and Mechanisms of the Pacific Decadal Oscillation in a Suite of Coupled Models from the Geophysical Fluid Dynamics Laboratory. Journal of Climate 28(19):7678–7701, https://doi.org/10.1175/JCLI-D-14-00647.1, https://journals.ametsoc.org/view/journals/clim/28/19/jcli-d-14-00647.1.xml, publisher: American Meteorological Society Section: Journal of Climate

Zhang R, Delworth TL (2005) Simulated Tropical Response to a Substantial Weakening of the Atlantic Thermohaline Circulation. J Clim 18(12):1853–1860. https://doi.org/10.1175/jcli3460.1

Zhang R, Delworth TL (2006) Impact of Atlantic multidecadal oscillations on India/Sahel rainfall and Atlantic hurricanes. Geophysical Research Letters 33(17), https://doi.org/10.1029/2006GL026267

Zhang Z, Chan JCL, Ding Y (2004) Characteristics, evolution and mechanisms of the summer monsoon onset over Southeast Asia. Int J Climatol 24(12):1461–1482. https://doi.org/10.1002/joc.1082

Zhou J, Lau KM (2001) Principal modes of interannual and decadal variability of summer rainfall over South America. Int J Climatol 21(13):1623–1644. https://doi.org/10.1002/joc.700

Zhou T, Yu R, Zhang J, Drange H, Cassou C, Deser C, Hodson DL, Sanchez-Gomez E, Li J, Keenlyside N, Xin X, Okumura Y (2009) Why the Western Pacific Subtropical High Has Extended Westward since the Late 1970s. J Clim 22(8):2199–2215. https://doi.org/10.1175/2008jcli2527.1

Zwiers FW (1996) Interannual variability and predictability in an ensemble of AMIP climate simulations conducted with the CCC GCM2. Clim Dyn 12(12):825–847. https://doi.org/10.1007/s003820050146